Model for the fragmentation of copper matte particles during flash converting

M. Pérez-Tello and I.M. Madrid-Ortega
Professor and research assistant, respectively, Departamento de Ingeniería Química y Metalurgia, Universidad de Sonora, Hermosillo, Sonora, Mexico

H.Y. Sohn
Professor, Department of Metallurgical Engineering, University of Utah, Salt Lake City, Utah

Abstract
A mathematical model to represent the expansion and fragmentation of copper matte particles oxidized under flash converting conditions is presented. The model assumes that the particles are initially nonporous, have a constant mass prior to fragmentation and travel at a constant velocity throughout the reaction chamber. The model requires the specification of the following five parameters: the particle expansion rate, a fragmentation diameter factor, a fragmentation size distribution parameter and the fractions of the finest and the coarsest particles in the feed that undergo fragmentation. The model predictions show good agreement with the experimental data collected in a laboratory furnace over a wide range of experimental conditions. The evolution of the size distribution of the particles along the reactor length was computed, and the model parameters were correlated with the experimental operating variables. Model predictions indicate that particle residence time is an important factor in the generation of dust. The presence of two maxima in the particle density function may be attributed to turbulent conditions prevailing in the furnace, which cause particles to follow different trajectories within the furnace even if they are injected at the same location.

Key words: Particle fragmentation, Flash converting, Copper matte, Mathematical modeling

Introduction
The oxidation of sulfide particles at high temperature is often accompanied by morphological and size changes. Typical examples include the flash smelting of copper and nickel concentrates and the flash converting of copper mattes. Although the reaction path of individual particles in these processes is still under debate, it is generally accepted (Kim and Themelis, 1986; Jokilaakso et al., 1991) that particles change in size as a result of bloating followed by fragmentation during their flight in the reaction chamber.

The study of particle fragmentation in flash smelting and flash converting processes is of practical interest because it is related to the generation of dust particles. Whereas large particles get fully molten in the reaction shaft and eventually reach the molten bath, small particles may be carried away by the process gas towards the uptake shaft, waste heat boiler and electrostatic precipitator. Although dust particles are usually recycled to the process, their presence is undesirable because they cause problems such as plugging of the transport system, corrosion and a decrease in steam production.

The development of mathematical models to describe the size changes experienced by sulfide particles during flash smelting and flash converting has received little attention in the literature. This is probably because of the difficulties encountered in the collection of data to validate such models. The present authors have conducted extensive experimentation on the flash converting of copper matte particles in a large laboratory furnace, which is shown in Fig. 1, at the University of Utah (Perez-Tello et al., 2001a). The facility consists of five units: a solid and gas feeding unit, a reaction shaft, a product receptacle, a sampling probe and an off-gas unit. The reaction shaft consists of a vertical, one-piece cast alumina ceramic cylinder with an inner diameter of 0.24 m, a height of 1.4 m and a wall thickness 0.025 m. Granulated and ground copper matte particles were stored in a hopper and fed into the furnace with a single-screw feeder. The process gas was supplied by two rotameters handling pure oxygen and air, respectively, at room temperature and pressure (298 K, and 86.1 kPa in Salt Lake City). The particle feed rate was 3 kg/h, and the gas flow rate was adjusted to satisfy the oxygen-to-matte ratio to be tested.

Paper number MMP-06-063. Original manuscript submitted October 2006. Revised manuscript accepted for publication March 2007. Discussion of this peer-reviewed and approved paper is invited and must be submitted to SME Publications Dept. prior to August 31, 2008.

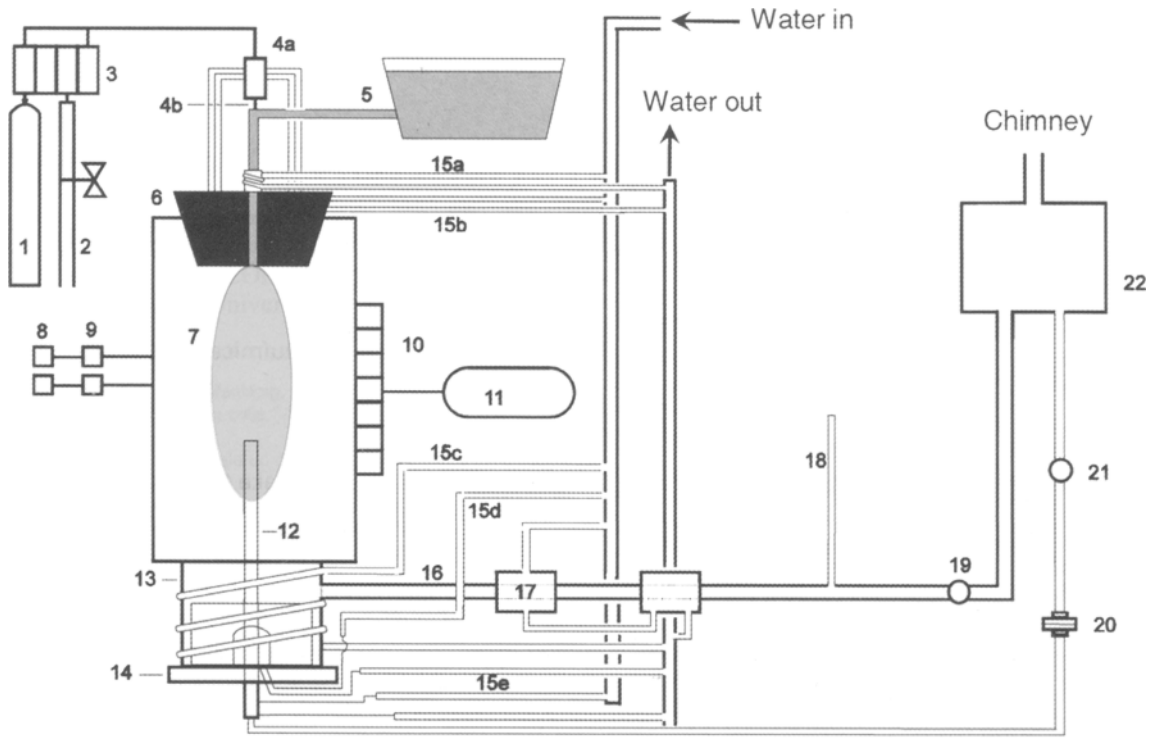

Figure 1 — Flash converting facility at the University of Utah.

The following two matte grades were used: high-grade matte particles containing 72% Cu by weight (which closely represents the matte processed in the commercial unit) and low-grade matte particles containing 58% Cu by weight. In a typical experiment, the particles and gas entered the furnace through a water-cooled Outokumpu-type pilot-scale burner. The particles were oxidized while flowing downwards with the gas and were collected in the receptacle, which was detachable and externally water-cooled by a copper coil. The goal of the receptacle was to quench the particles falling from the shaft, thus interrupting the oxidation reactions, and collect them for further analysis. Input variables tested in the experiments included the particle size of the feed, oxygen concentration (OC) in the process gas and the oxygen-to-matte ratio (OMR). Response variables measured in the particles included the chemical analysis in terms of copper, iron and sulfur contents; the morphology and mineralogy of the reacted particles; and the size distribution of the particle population under various experimental conditions.

A thorough discussion of the experimental data is presented elsewhere (Perez-Tello et al., 2001a). Overall, substantial differences in the oxidation behavior of particles from the two mattes were observed. The low-grade (58% Cu) matte particles reacted evenly throughout the reaction chamber, increased in size and experienced no substantial fragmentation during oxidation. In contrast, the high-grade (72% Cu) matte particles oxidized unevenly in the reaction shaft and experienced severe fragmentation leading to substantial generation of dust. Whereas most of the chemical changes experienced by the particles were reasonably explained in terms of a comprehensive mathematical model (Perez-Tello et al., 2001b), the size changes experienced by the particles were not included in the formulation. In a subsequent paper (Perez-Tello et al., 2002), the authors developed mathematical correlations to describe the size distribution in both the feed and the receptacle of the laboratory furnace. Although the accuracy of such correlations was found to be satisfactory, they cannot be used to analyze particle fragmentation from a fundamental standpoint.

The goal of this investigation was twofold: to develop a simple mathematical model capable of describing with reasonable accuracy the particle size changes of high-grade, 72% Cu matte particles during oxidation in the laboratory furnace at the University of Utah and to use this model to explain the changes in the size distribution of particles during oxidation in the reaction shaft of the laboratory furnace.

Model formulation and numerical solution

The present model is shown schematically in Fig. 2 and is based on the qualitative model reported in the literature (Jokilaakso et al., 1991). The following assumptions were made:

- the particles are initially nonporous,
- the particles travel at a constant velocity throughout the reaction chamber and
- the particles have a constant mass prior to fragmentation.

Other assumptions are described below.

The first assumption above is consistent with microscopic observations of the initial particles (Perez-Tello et al., 2001a). The second assumption is based on computational fluid dynamic (CFD) calculations (Perez-Tello et al., 2001b), which showed that turbulent conditions in the laboratory furnace were restricted within 600 mm below the burner tip, whereas the rest of the chamber behaved as a plug-flow reactor. The third assumption is the main restriction of the present formulation. Because the goal of this investigation was to initiate the study of particle fragmentation from a fundamental standpoint, as a first step, the reaction kinetics was not considered to keep the formulation within a reasonable mathematical complexity.

Future work will be aimed at incorporating a kinetic model for the converting reactions (Perez-Tello et al., 2001b) into the present formulation to assess the effects of the chemical reactions on particle fragmentation.

A starting copper matte particle with initial size x_{i0} is assumed to expand at a constant rate g, so that its size x_i at time t will be

$$x_i = x_{i0} + gt \qquad i = 1, n \tag{1}$$

where

subscript i indicates the i^{th} size fraction in the feed and

n is the total number of size fractions.

The particle expansion rate g was assumed to be independent of particle size. During the flight, the particle expands until it reaches a critical size x_{ic}, which is dependent on the initial size fraction

$$x_{ic} = f_c x_{i0} \qquad i = 1, n \tag{2}$$

where

f_c is a proportionality constant.

Because particles of the same size fraction may have different trajectories inside the reaction chamber under turbulent conditions, fraction f_{if} of the population of particles with initial size x_{i0} was assumed to achieve fragmentation, whereas the remaining $(1 - f_{if})$ was assumed to continue expansion until reaching the receptacle.

Because the particles were quickly cooled in the lower portion of the furnace, it was assumed that no fragmentation occurred in the receptacle. This hypothesis is supported by CFD calculations (Perez-Tello et al., 2001b), which showed that the particle temperature just above the receptacle (800K) was significantly lower than the temperature in the reaction zone (1,650K).

The time spent by the particles to reach their critical size x_{ic} is denoted by t_{ic} and can be computed from Eq. (1) by setting $x_i = x_{ic}$. Let f_i be the fraction of particles of size x_{i0} that have fragmented by time t. Fragmentation was assumed to occur gradually along the particle trajectory according to

$$f_i = \frac{(t - t_{ic})}{(\tau - t_{ic})} f_{if} \qquad \text{i} = 1, n \tag{3}$$

where

$\tau = L/v$ is the mean residence time of the particles,

L is the reactor length and

v is the particle velocity.

In this study, v = 2.3 m/s and L = 2 m (Perez-Tello et al., 2001b). Equation (3) satisfies the conditions: $f_i = 0$ for $t = t_{ic}$ and $f_i = f_{if}$ for $t = \tau$. The fraction of particles that have fragmented by the time they reach the receptacle was assumed to obey the following linear relationship with the initial particle size

$$f_{if} = f_{2f} + \left(\frac{f_{nf} - f_{2f}}{x_{n0} - x_{20}} \right) (x_{i0} - x_{20}) \qquad i = 2, n \tag{4}$$

where

f_{2f} and f_{nf} refer to fractions of the initial sizes x_{20} and x_{n0}, respectively.

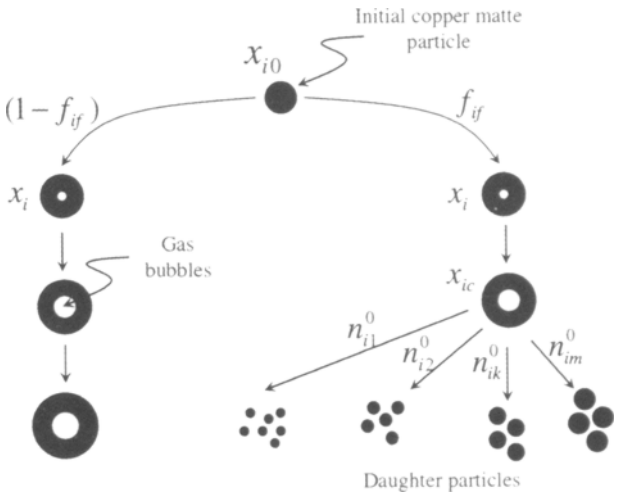

Figure 2 — Schematic representation of the fragmentation model.

Size x_{20} is the second smallest in the feed. For numerical purposes, the smallest fraction in the feed, x_{10}, was assumed not to fragment. Similarly, the largest fraction in the feed, x_{n0}, was assumed not to expand. The fragmentation was assumed to produce nonporous daughter particles of sizes x_{k0}, where $k = 1, i - 1$.

Because reaction kinetics was not considered in the present formulation, the mass density of the daughter particles was assumed to be equal to that of the initial particle; therefore, $x_{k0} < x_{i0}$. Let n_{ik}^0 be the number of particles of size x_{k0} produced from a single particle of size x_{i0}. The number of daughter particles produced from the starting particle is denoted by n_i^0 and is given by

$$n_i^0 = \sum_{k=1}^{i-1} n_{ik}^0 \qquad i = 1, n \tag{5}$$

Let $\lambda_{ik} = n_{ik}^0 / n_i^0$ be the fragmentation ratio. Substituting this expression into Eq. (5) yields

$$\sum_{k=1}^{i-1} \lambda_{ik} = 1 \qquad i = 1, n \tag{6}$$

The fragmentation ratio λ_{ik} was modeled by

$$\lambda_{ik} = k_i \left(\frac{x_{k0}}{x_{i0}} \right)^{\gamma} \qquad i = 1, n \tag{7}$$

where

k_i is a proportionality constant and γ is a distribution parameter.

Equation (7) is similar to the empirical expressions used to compute the selection function in batch comminution operations (King, 1973). Parameter γ indicates the distribution of sizes on fragmentation. When $\gamma < 0$, the initial particle produces fine daughter particles; when $\gamma = 0$, the fragments distribute

uniformly into all size fractions; finally, when $\gamma > 0$, the initial particle produces large daughter particles. Because γ was set to be independent of particle size, particles of all sizes were assumed to fragment similarly. On substituting Eq. (7) into Eq. (6), the following expression is obtained

$$k_i = \frac{1}{\sum_{k=1}^{i-1}\left(\frac{x_{k0}}{x_{i0}}\right)^{\gamma}} \qquad i = 1, n \qquad (8)$$

Thus, parameter k_i can be computed from Eq. (8) and can further be used to compute λ_{ik} from Eq. (7). Upon fragmentation, the mass of the initial particle is distributed throughout the daughter particles.

Because all the particles are assumed to be spherical and have equal densities, the mass conservation relationship reduces to the volume-conservation expression

$$x_{i0}^3 = \sum_{k=1}^{i-1} n_{ik}^0 x_{k0}^3 \qquad i = 1, n \qquad (9)$$

Substitution of $\lambda_{ik} = n_{ik}^0/n_i^0$ into Eq. (9) yields, on rearrangement

$$n_i^0 = \frac{x_{i0}^3}{\sum_{k=1}^{i-1} \lambda_{ik} x_{k0}^3} \qquad i = 1, n \qquad (10)$$

The number of particles of size x_{k0} produced by all the particles of initial size x_{i0} that achieved fragmentation at time t is given by

$$n_{ik} = n_{ik}^0 n_i f_i \qquad i = 1, n \qquad (11)$$

where

n_i is the number of particles of size x_{i0} in the feed to the reactor and is computed from

$$n_i = \frac{f_3(x_{i0})(\Delta x_{i0})W}{\rho_0 C_3 x_{i0}^3} \qquad i = 1, n \qquad (12)$$

where

$f_3(x_{i0})$ is the mass density function of size fraction x_{i0} in the feed,

Δx_{i0} is the size interval,

W is the total mass of all the particles of all sizes being fed to the furnace,

$\rho_0 = 5{,}400$ kg/m^3 is the particle density and

$C_3 = \pi/6$ is the particle shape factor.

Equation (12) represents the total mass of particles of size x_{i0} in the feed divided by the mass of a single particle of size x_{i0}.

The mass of particles of size x_{k0}, which were produced by the fragmentation of all particles of starting size x_{i0}, where $x_{i0} > x_{k0}$ at time t is given by

$$m_{ik} = n_{ik}\rho_0 C_3 x_{k0}^3 \qquad i = k+1, n \qquad (13)$$

Similarly, the mass of particles of size x_{k0}, which resulted from the expansion of all particles of starting size x_{l0}, where $x_{l0} < x_{k0}$ at time t, is given by

$$m_{lk} = (1 - f_l) n_l \rho_0 C_3 x_{l0}^3 \qquad l = 1, k-1 \qquad (14)$$

Therefore, the total mass of particles of size x_{k0} at time t is given by the summation of Eqs. (13) and (14) and is denoted by m_k

$$m_k = \sum_{l=1}^{k-1} m_{lk} + \sum_{i=k+1}^{n} m_{ik} \qquad k = 1, n \qquad (15)$$

Finally, the mass density function of size fraction x_{k0} at time t is given by

$$f_3(x_{k0}) = \frac{m_k}{\left(\sum_{k=1}^{n} m_k\right)\Delta x_k} \qquad k = 1, n \qquad (16)$$

Equation (16) is the final relationship to compute the size distribution of particles in the reaction chamber. When $t < \tau$, $f_3(x_{k0})$ represents the size distribution along the reactor length, whereas for $t = \tau$, it represents the size distribution in the receptacle of the laboratory furnace. The mathematical model can be fully solved by specifying five parameters: g, f_c, γ, f_{2f} and f_{nf}. As further theory/experiments on the fragmentation of particles become available, the formulation may be extended to incorporate the functionality of all the model parameters with particle size.

The parameter values were determined by the following iterative procedure. First, the experimental size distributions in the feed and the receptacle were represented, respectively, by the empirical expressions

$$f_3(x) = bx^c e^{-ax} \qquad (17)$$

and

$$g_3(x) = b_1 x^{c_1} e^{-a_1 x} + b_2 x^{c_2} e^{-a_2 x} \qquad (18)$$

Parameters a and b in Eqs. (17) and (18) were reported by the authors (Perez-Tello et al., 2002). Equation (17) is the starting point to calculate the number of particles in every size fraction in the feed according to Eq. (12). For every size fraction, its trajectory along the reaction chamber was computed.

On reaching the receptacle, the r^2 correlation parameter was computed

$$r^2 = 1 - \frac{\sum_{i=1}^{n}\left[g_3(x_i) - f_3(x_i)\right]^2}{\sum_{i=1}^{n}\left[g_3(x_i) - \overline{g_3(x_i)}\right]^2} \qquad (19)$$

where

$g_3(x_i)$ is the i^{th} experimental value from Eq. (18),

$f_3(x_i)$ is the i^{th} predicted value from Eq. (16),

$\overline{g_3(x_i)}$ is the mean experimental value and

n is the number of size fractions in the population.

In this study, n was set to 300. The model parameters were varied in consecutive iterations until the r^2 value was as close to unity as possible.

Discussion of results

Table 1 summarizes the numerical values of the model parameters obtained for all the experimental conditions. Because the fractions labels (<37, 37-74, etc.) do not exactly correspond to the actual particle sizes within those fractions, the mean size reported in Table 1 was computed from

$$\langle x \rangle_f = \int_0^{\infty} x f_{3,e}(x) dx \qquad (20)$$

where

$f_{3,e}(x)$ is the experimental particle density function in the feed.

The average r^2 value in Table 1 is 0.914. Thus, overall, there was good agreement between the predicted and the experimental values.

It is of interest to note the ranges of the model parameters because they have physical implications. They are summarized in Table 2. To the best of the authors' knowledge, the values in

Table 1 — Experimental conditions and numerical values of the parameters in the fragmentation model.

Run	Size fraction in the feed, μm	Feed mean size, $\langle x \rangle_f$, μm	Oxygen-to-matte ratio (OMR), kg O_2/kg matte	Oxygen concentration (OC) in process gas, Vol. %	g μm/s	γ	f_{2f}	f_{nf}	f_c	r^2
1	<37	42.6	0.25	70	55.0	-0.50	0.55	0.55	1.20	0.960
2	<37	42.6	0.33	70	45.0	-1.95	0.80	0.80	1.20	0.980
3	<37	42.6	0.25	100	55.0	-1.60	0.75	0.23	1.20	0.992
4	<37	42.6	0.33	100	55.0	-2.20	0.69	0.15	1.20	0.981
5	37-74	67.6	0.25	70	20.0	-2.70	0.36	0.90	1.12	0.981
6	37-74	67.6	0.33	70	40.0	-2.90	0.60	1.00	1.20	0.900
7	37-74	67.6	0.25	100	21.0	-2.82	0.50	0.50	1.10	0.959
8	37-74	67.6	0.33	100	40.0	-2.90	0.79	0.79	1.20	0.925
9	74-105	103.5	0.25	70	5.0	-3.40	0.20	1.00	1.02	0.849
10	74-105	103.5	0.33	70	18.0	-3.30	0.50	0.99	1.05	0.805
11	74-105	103.5	0.25	100	5.0	-3.40	0.20	1.00	1.02	0.831
12	74-105	103.5	0.33	100	28.0	-3.30	0.50	0.99	1.10	0.838
13	105-149	130.6	0.25	70	3.5	-3.50	0.20	0.95	1.02	0.767
14	105-149	130.6	0.33	70	13.0	-3.20	0.50	0.80	1.06	0.954
15	105-149	130.6	0.25	100	5.0	-3.40	0.20	0.95	1.02	0.888
16	105-149	130.6	0.33	100	13.0	-3.30	0.45	0.80	1.06	0.905
17	<149	74.9	0.25	70	53.0	-2.50	0.10	0.80	1.15	0.983
18	<149	74.9	0.33	70	50.0	-2.90	0.34	0.90	1.15	0.936
19	<149	74.9	0.25	100	60.0	-3.10	0.18	0.80	1.20	0.908
20	<149	74.9	0.33	100	50.0	-2.90	0.40	0.90	1.10	0.944

Table 2 are the first attempt to represent on a quantitative basis the relevant factors involving particle fragmentation in flash converting. The following features are observed:

- with the exception of the critical size parameter f_c, all the parameters show a relatively large range of variation, which is attributable to the varying experimental conditions;
- all the particles experienced expansion because $g > 0$ in all cases;
- on fragmentation, particles significantly smaller than their original sizes are produced, i.e., $\gamma < 0$ in all cases;
- large particles in the feed have higher probability to get fragmented than small particles; this is noted because the upper limit of f_{nf} is unity, whereas the upper limit for f_{2f} is 0.79; and
- the fragmentation of particles initiates within a relatively short time on entering the reaction chamber; i.e., the f_c values indicate that particles only increase by 2% to 20% of their initial size prior to the start of fragmentation.

Figures 3a and 3b show the results obtained with the present model and their comparison with the experimental data for Runs 7 and 15, respectively. Overall, a reasonable agreement between the predicted and the experimental values is noted. Figures 4a and 4b show the predicted and experimental values for Runs 17 and 20, respectively, in which the feed to the reactor was not sieved. Runs 17 and 20 thus represent situations most similar to an industrial operation. Figures 4a and 4b show that despite this difficulty, the model was able to predict the size distribution in the receptacle with reasonable accuracy. A significant feature of the present formulation is its capability to reproduce the two maxima in the particle size distribution of the reacted products, as is noted in Figs. 3a, 3b, 4a and 4b. This feature is predicted by parameter f_{if}. When f_{if} is set equal to either zero or unity, the size distribution is predicted to have a single maximum. Therefore, the two maxima in the size distribution of the reacted products may be attributed to the turbulent conditions prevailing in the furnace, which causes identical particles injected at the same location to follow different trajectories along the reaction shaft.

Figure 5 shows the predicted evolution of the particle size distribution along the reactor length for Run 17. The size distribution in the feed presents a single maximum at 46 μm. As a result of particle expansion, this maximum gradually shifts towards the coarsest sizes as particles travel through the reaction chamber. A second maximum at about 22 μm, i.e., in the range of fine dust particles, also starts forming during particles flight. The second maximum results from the fragmentation of some of the particles that previously expanded at higher positions in the furnace. Figure 5 suggests that the amount of dust produced in the furnace is dependent on the time spent by the particles in the reaction chamber.

Figures 6 through 10 show the overall sensitivity of the model parameters with the operating conditions in the laboratory furnace. A noticeable feature is the behavior of the unsieved material <149 μm, which in all cases deviated from the behavior of the sieved size fractions. The experiments with the unsieved material are represented by the symbols not connected to other symbols along the continuous lines. The wide distribution of sizes in the unsieved material is likely to be responsible for these results. Thus, the mean size $\langle x \rangle_f$ was not sufficient to

Table 2 — Ranges of variation of the model parameters.

Parameter	Range
g	5 to 60 μm/s
γ	-3.5 to -0.5
f_{2f}	0.1 to 0.79
f_{nf}	0.15 to 1.0
f_c	1.02 to 1.2

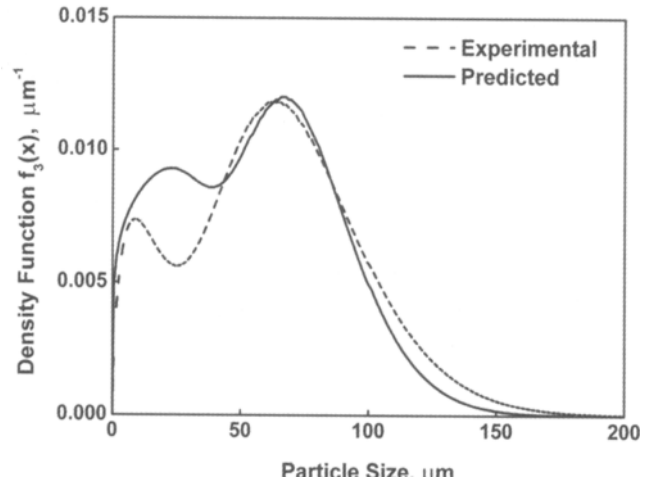

Figure 3a — Experimental and predicted particle size distribution in the receptacle of the laboratory flash converting furnace for Run 7 in Table 1.

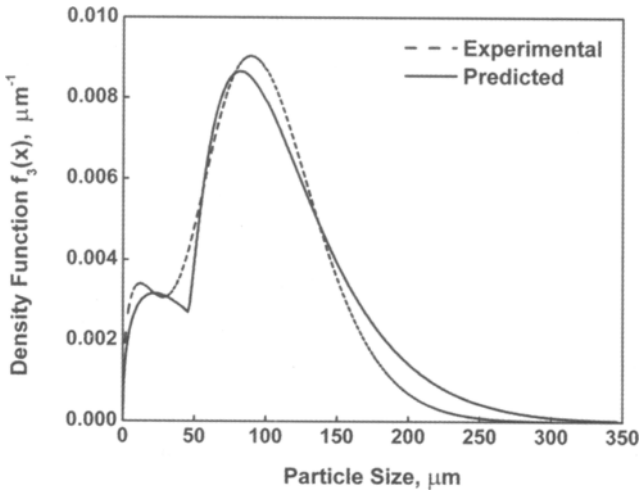

Figure 4a — Experimental and predicted particle size distribution in the receptacle of the laboratory flash converting furnace for Run 17 in Table 1.

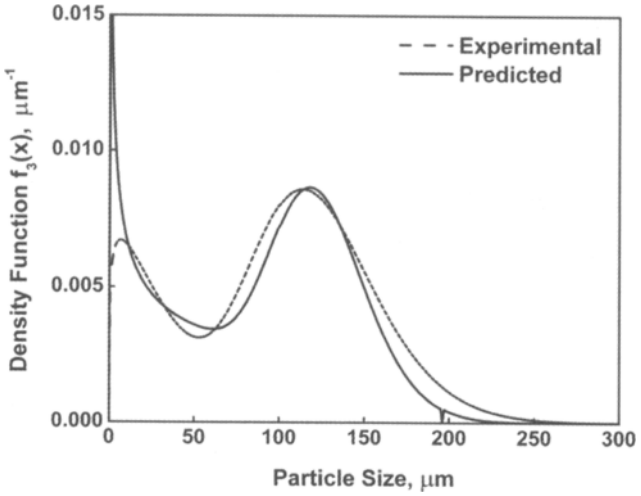

Figure 3b — Experimental and predicted particle size distribution in the receptacle of the laboratory flash converting furnace for Run 15 in Table 1.

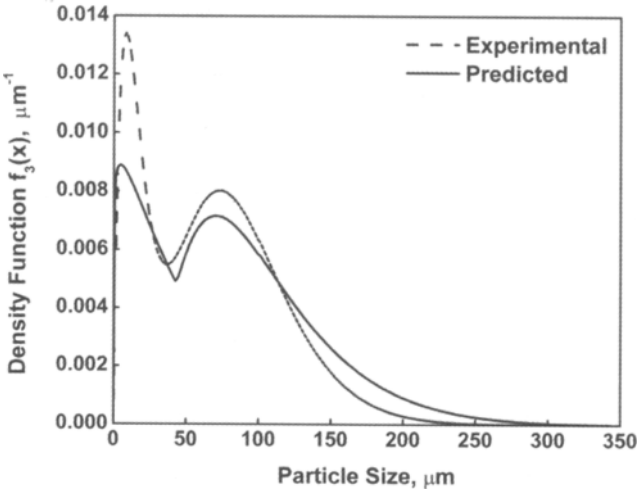

Figure 4b — Experimental and predicted particle size distribution in the receptacle of the laboratory flash converting furnace for Run 20 in Table 1.

represent the particle population, and the incorporation of the variance may be necessary.

Figure 6 shows that f_c decreases as $\langle x \rangle_f$ increases, i.e., large particles do not expand significantly prior to fragmentation. Also, as the OMR increases the value of f_c increases, whereas OC does not seem to play a significant role. Such trends are consistent with the experimental observations (Perez-Tello et al., 2001a) in which OMR and $\langle x \rangle_f$ mostly affected particle fragmentation. Figure 7 shows that particle expansion rate g decreases as $\langle x \rangle_f$ increases, i.e., small particles expand faster than large particles. This result agrees with the microscopic examination of the reacted particles (Perez-Tello et al., 2001a). Also, as the OMR increases, the value of g increases. The higher reactivity of the particles observed at high OMR may explain this trend. When the amount of oxygen provided to the particles exceeds the stoichiometric amount of 0.25 kg O_2/kg matte, the formation of copper oxides in the particles becomes feasible. Finally, oxygen concentration (OC) does not play a significant role on the g values. This also agrees with the experimental observations in which OC did not significantly affect the particle reactivity and particle fragmentation.

The size distribution parameter γ (Fig. 8) decreases as $\langle x \rangle_f$ increases, and it approaches the asymptotic value of $\gamma \approx -3.25$ for $\langle x \rangle_f > 67.6$ μm. The finest particles in the feed were most sensitive to the operating conditions, as the values of γ for $\langle x \rangle_f =$ 42.6 μm vary in the range of -0.5 to -2.2. According to Eq. (7), such a large range of variation makes a substantial difference in the distribution of daughter particles upon fragmentation.

In general, f_{2f} decreases as $\langle x \rangle_f$ increases and becomes asymptotic for $\langle x \rangle_f > 103.5$ μm, as is shown in Fig. 9. Overall, the larger the size of the accompanying particles the less extensive fragmentation of the smallest particles in the feed. Also, f_{2f} increases as the OMR increases. This trend is consistent with the experimental observations in which an increase in the OMR produced a significant increase in the fragmentation of particles under all experimental conditions. The fraction of the

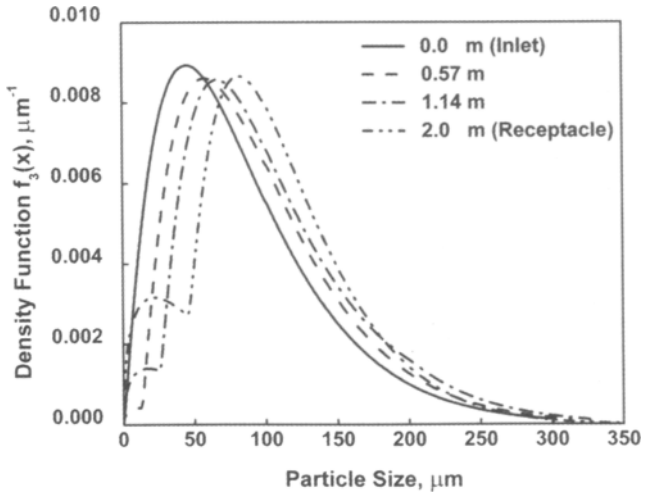

Figure 5 — Predicted evolution of the particle size distribution along the reaction shaft in the laboratory furnace, run 17. Label numbers indicate distance from the inlet.

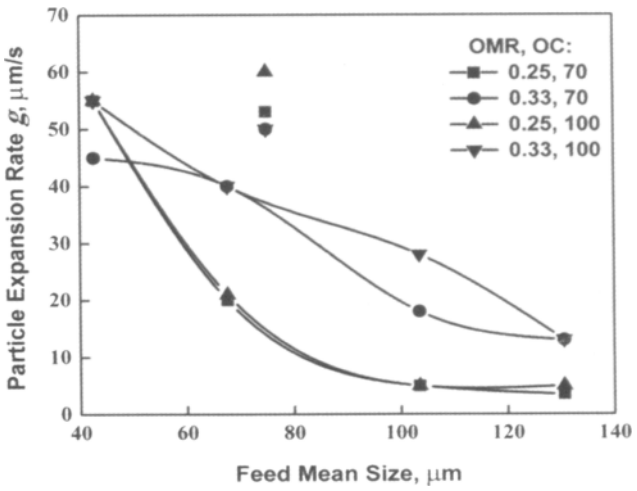

Figure 7 — Particle expansion rate as a function of the feed mean size, oxygen-to-matte ratio (OMR) and oxygen concentration (OC).

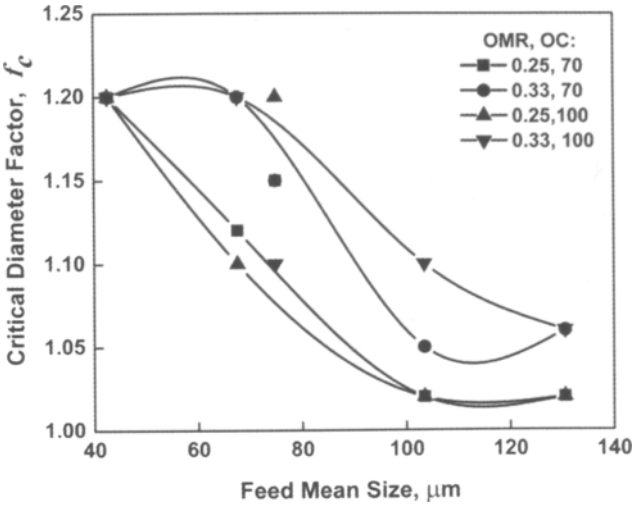

Figure 6 — Critical diameter factor as a function of the feed mean size, oxygen-to-matte ratio (OMR) and oxygen concentration (OC).

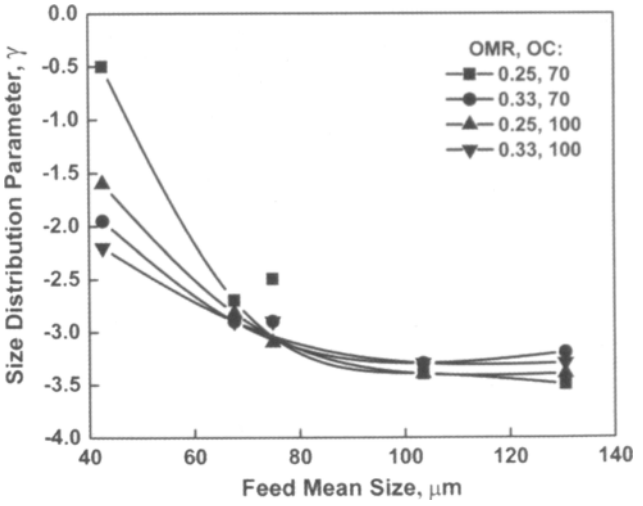

Figure 8 — Size distribution parameter as a function of the feed mean size, oxygen-to-matte ratio (OMR) and oxygen concentration (OC).

coarsest particles that undergo fragmentation is shown to be a strong function of $\langle x \rangle_f$, especially in the range of $42.6 < \langle x \rangle_f < 103.5$ μm (Fig. 10). It is of interest to note that f_{nf} increases up to $\langle x \rangle_f = 103.5$ μm regardless of the OMC and OC values. Thus, the larger the size of the accompanying particles, the more extensive is the fragmentation of the coarsest particles in the feed. The effects of the OMR and OC on f_{nf} are significant when $\langle x \rangle_f < 103.5$ μm, whereas for larger values of $\langle x \rangle_f$, the OMR and OC do not seem to play a significant roles.

The fact that both f_{2f} and f_{nf} are dependent on the mean size of the feed suggests that the turbulent conditions faced by the particles are affected by the presence of other particles in the feed. This observation is consistent with CFD calculations of the laboratory furnace (Perez-Tello et al., 2001b) that showed that gas and particle equations are highly coupled in this type of a system. The coupling is due to the large mass of particles in the particle-gas suspension (roughly 74% by weight), which contrasts with the small volume occupied by the particles (typically less than 0.01% by volume). Under such conditions, particle-gas interactions are strong, whereas particle-particle interactions are very unlikely. Further CFD calculations may help clarify this issue and provide physical interpretation to the trends observed in Figs. 9 and 10.

An overall evaluation of the present formulation indicates that a reasonable agreement between the predicted and the experimental values was obtained. The largest deviations were observed in the range of 0 to 25 μm, as was noted in Figs. 3a, 3b, 4a and 4b. The experimental curves in this range typically showed very steep, narrow peaks, which are difficult to reproduce by numerical calculations. In the experiments, dust particles in the range of zero to 25 μm were mostly made up by copper oxides (Perez-Tello et al., 2001a). Because copper oxides and copper matte densities are substantially different, it is likely that this discrepancy may be attributed to the model assumption that particles have equal densities before and after fragmentation. The fact that this simplification led to overall reasonable results

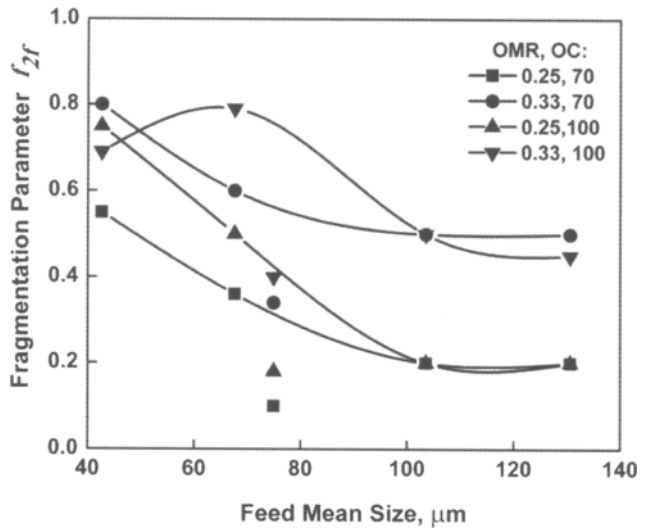

Figure 9 — Fragmentation parameter f_{2f} as a function of the feed mean size, oxygen-to-matte ratio (OMR) and oxygen concentration (OC).

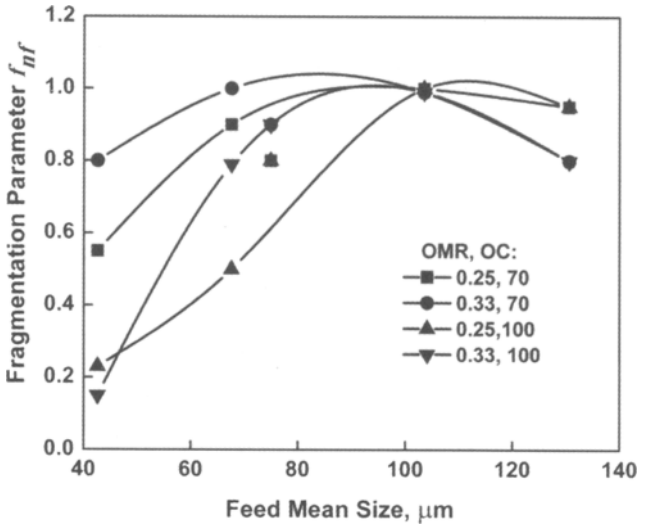

Figure 10 — Fragmentation parameter f_{nf} as a function of the feed mean size, oxygen-to-matte ratio (OMR) and oxygen concentration (OC).

suggests that, on fragmentation, most of the daughter particles retained the chemical composition of their mother particle. The exception is the fine dust particles that may originate in the oxide crust surrounding the sulfide core of the mother particle (Jokilaakso et al., 1991). The incorporation of a kinetic model into the present formulation will help clarify this issue, and will be the subject of future work by the authors.

Concluding remarks

A predictive mathematical model for the expansion and fragmentation of copper matte particles oxidized under flash converting conditions is presented. The model requires the specification of five parameters, all of which have physical significance. The model predictions show good agreement with the experimental data collected in a large laboratory furnace. A relevant feature of the present formulation is its capability to reproduce the two maxima in the particle size distribution. This was attributed to the turbulent conditions prevailing in the furnace, which cause particles to follow different trajectories within the furnace even if they are injected at the same location.

The formation of dust particles was found to be dependent on the residence time of the particle population in the reaction chamber. The dependency of the model parameters on the operating conditions in general agreed with the trends observed in the experiments and with CFD calculations previously reported by the authors. Direct verification of the applicability of the present model to the industrial operation must await the availability of reliable data.

References

Jokilaakso, A.T., Suominen, R.O., Taskinen, P.A., and Lilius, K.R., 1991, "Oxidation of chalcopyrite in simulated suspension smelting," *Transactions of the Institution of Mining and Metallurgy, Section C – Mineral Processing and Extractive Metallurgy*, Vol. 100, pp. C79-C90.

Kim, Y.H., and Themelis, N.J., 1986, "Effect of phase transformation and particle fragmentation on the flash reaction of complex metal sulfides," *The Reinhardt Schuhmann International Symposium on Innovative Technology and Reactor Design in Extractive Metallurgy*, D.R. Gaskell, Hager, J.P., Hoffman, J.E., Mackey, P.J., eds., Nov. 9-12, 1986, Colorado Springs, Colorado, TMS, Warrendale, Pennsylvania, pp. 349-369.

King, R. P., 1973, "An analytical solution to the batch comminution equation," *Journal of South African Institute of Mining and Metallurgy*, Vol. 73, pp. 127.

Perez-Tello, M., Sohn, H.Y., St Marie, K., and Jokilaakso, A., 2001a, "Experimental investigation and three-dimensional computational fluid-dynamics modeling of the flash-converting furnace shaft: Part I. Experimental observation of copper converting reactions in terms of converting rate, converting quality, changes in particle size, morphology, and mineralogy," *Metallurgical and Materials Transactions B – Process Metallurgy and Materials Processing Science*, Vol. 32, No. 5, pp. 847-868.

Perez-Tello, M., Sohn, H.Y., and Smith, P.J., 2001b, "Experimental investigation and three-dimensional computational fluid-dynamics modeling of the flash-converting furnace shaft: Part II. Formulation of three-dimensional computational fluid-dynamics model incorporating the particle-cloud description," *Metallurgical and Materials Transactions B – Process Metallurgy and Materials Processing Science*, Vol. 32, No. 5, pp. 869-886.

Perez-Tello, M., Tirado-Ochoa, J.A., Sohn, H.Y., and Sánchez-Corrales, V.M., 2002, "Size distribution analysis of copper matte particles oxidized under flash converting conditions," *JOM*, Vol. 54, No. 10, pp. 27-30.